



Cite this: *Dalton Trans.*, 2015, 44, 15387

Received 19th June 2015,  
Accepted 27th July 2015

DOI: 10.1039/c5dt02340h

www.rsc.org/dalton

## Application of the $\pi$ -accepting ability parameter of N-heterocyclic carbene ligands in iridium complexes for signal amplification by reversible exchange (SABRE)<sup>†</sup>

Bram J. A. van Weerdenburg, Nan Eshuis, Marco Tessari, Floris P. J. T. Rutjes and Martin C. Feiters\*

The new  $\pi$ -accepting ability parameter (PAAP) appears to be the best tool to analyse the electronic properties of NHC ligands in  $[\text{Ir}(\text{H})_2(\text{NHC})(\text{Py})_3]^+$  complexes for SABRE. Together with the buried volume, the efficiency of hyperpolarisation transfer in SABRE, depending on the exchange rate of pyridine, can be described.

NMR is a powerful analytical tool that is widely used in the fields of chemistry, material science, and medicine. Because of the small population differences between the nuclear spin states in a magnetic field, however, NMR is intrinsically a relatively insensitive technique. This relative insensitivity can be overcome by using hyperpolarisation techniques to produce non-Boltzmann spin-state distributions. A promising approach is Signal Amplification By Reversible Exchange (SABRE), which was first described by Duckett *et al.*<sup>1</sup> In this method hyperpolarisation is achieved by the temporary association of a substrate and  $p\text{-H}_2$  in the coordination sphere of a transition metal, whereupon polarisation can be transferred from the  $p\text{-H}_2$ -derived hydride ligands to the bound substrate *via* scalar coupling (Fig. 1).<sup>2</sup> The hyperpolarised substrate then dissociates into the solution resulting in strongly enhanced NMR signals of its unbound form.

Since the discovery of SABRE, several small molecules,<sup>3,4</sup> mainly aromatic nitrogen heterocycles,<sup>5–8</sup> have been successfully hyperpolarised. However, for the development of the SABRE technique to a level where NMR can also be used for biomedical (imaging) applications some further problems must be addressed. Recently, much progress has been made, including the development of 2D-NMR methods,<sup>6</sup> analytical applications,<sup>9,10</sup> quantification methods,<sup>11</sup> and compatibility with high magnetic fields<sup>12–14</sup> and aqueous media.<sup>15–17</sup> In this

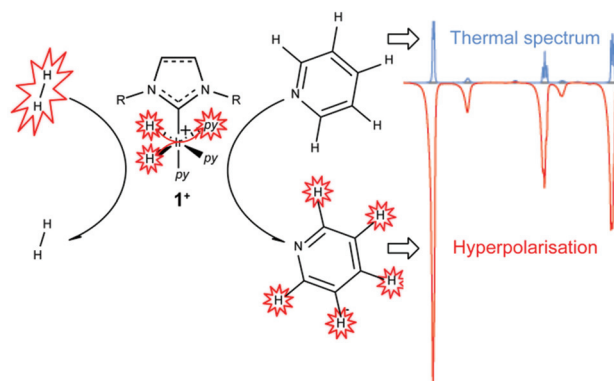


Fig. 1 Schematic representation of SABRE with the Ir catalyst  $1^+$  and pyridine (py) as the substrate.

perspective, development and optimisation of heterogeneous<sup>18,19</sup> and homogeneous catalysts<sup>20–25</sup> are also important; detailed insight in the catalytic process can lead to a more rational design of the next generation of catalysts.

We reported earlier<sup>20</sup> on the influence of the steric and electronic properties of NHC ligands in iridium complexes for SABRE as quantified by the buried volume ( $\%V_{\text{bur}}$ )<sup>26,27</sup> and an analogue of the Tolman Electronic Parameter (TEP), respectively (Fig. 2).<sup>28</sup> We measured the performance of the catalyst in terms of pyridine signal enhancement and exchange rate. The TEP had little distinguishing power in this series of NHC ligands, and there appeared to be no correlation with the chemical shift, exchange rate, or hyperpolarisation of pyridine. Inversely, the exchange rate increases generally with  $\%V_{\text{bur}}$ , which is consistent with a dissociative mechanism for the exchange of pyridine. The Ir-complex with IMes **5** had the optimum value for exchange rate and  $\%V_{\text{bur}}$ , resulting in the highest enhancement factor.<sup>20,21</sup> We also postulated that the property that has the strongest influence on the enhancement factor is the aromatic character of the substituent.

Radboud University, Institute for Molecules and Materials, Heyendaalseweg 135, 6525 AJ Nijmegen, The Netherlands. E-mail: m.feiters@science.ru.nl;

Fax: +31 24 36 53393; Tel: +31 24 36 52016

<sup>†</sup> Electronic supplementary information (ESI) available: General procedures and synthetic details. CCDC 1402867. For ESI and crystallographic data in CIF or other electronic format see DOI: 10.1039/c5dt02340h



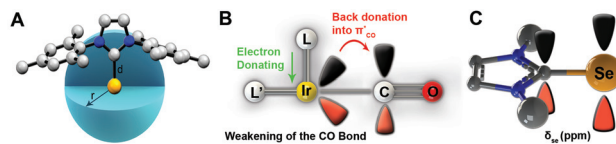


Fig. 2 Schematic representation of the used parameters; (A) buried volume (% $V_{bur}$ ), (B) Tolman Electronic Parameter (TEP), and (C) the  $\pi$ -accepting ability parameter (PAAP).

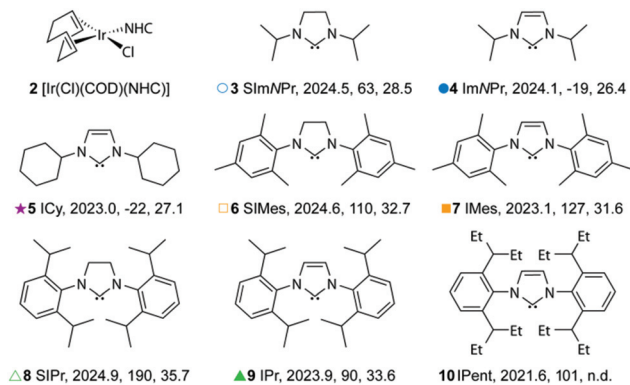


Fig. 3 Complex precursor and structure of NHC ligands, compound number, abbreviation, TEP ( $\text{cm}^{-1}$ ), PAAP ( $\delta_{se}$ , ppm), buried volume (%).

The contribution of the  $\pi$ -accepting ability of the NHC ligand to the metal-NHC bond has been recognised for some time,<sup>29</sup> and a new electronic parameter to describe this ability was developed only recently by Nolan, Cavallo and co-workers.<sup>30</sup> They defined the  $\pi$ -accepting ability parameter (PAAP) as the  $^{77}\text{Se}$  chemical shift of the corresponding selenourea complex and established the theoretical groundwork (Fig. 2). In addition, they predicted that this parameter can be deployed for characterisation and quantification of the  $\pi$ -accepting ability of existing and new NHC ligands. Here we will apply this new parameter to investigate the influence of the  $\pi$ -accepting ability of NHC ligands on the catalytic hyperpolarisation transfer in SABRE.

We have previously synthesised a series of [Ir(Cl)(COD)-(NHC)] complexes **2** (Fig. 3), which form the active SABRE complexes [Ir(H)<sub>2</sub>(NHC)(Py)<sub>3</sub>]<sup>+</sup> 1<sup>+</sup> upon addition of pyridine and hydrogen, and evaluated their performance in the hyperpolarisation of pyridine with an automated setup; the lifetime of the complex was determined by measuring the exchange rate of pyridine with the help of selective inversion recovery experiments.<sup>20</sup> Compared to our initial series of catalysts, ItBu is not included here, as its extremely high  $^{77}\text{Se}$  chemical shift ( $\delta_{se}$  183 ppm) was already considered an anomaly in the original correlation study of Cavallo *et al.* (see ESI†).<sup>30</sup> We started the evaluation of the PAAP by plotting the signal enhancement against the corresponding  $\delta_{se}$  of the ligands. As with the buried volume and TEP, this could not be correlated to the signal enhancement (not shown), however, this parameter

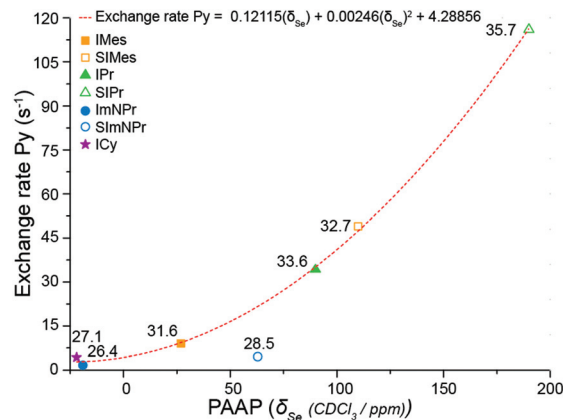


Fig. 4 Correlation between the exchange rate of pyridine and the  $\pi$ -accepting ability of ligands. Data points are labelled with the corresponding % $V_{bur}$ .

seems to correlate to a certain extent to the observed exchange rates as depicted in Fig. 4.

We have shown earlier<sup>20</sup> that in general a higher steric bulk leads to a higher exchange rate. While unsaturated ligands (*e.g.* ImNPr **4**, IMes **7**) have slightly less steric bulk than their saturated analogues (*e.g.* SiMnPr **3**, SIMes **6**), these subtle differences did not properly explain the large differences in the observed exchange rate; imidazolium derived ligands had exchange rates that are approximately 3–5 times larger than those of their saturated counterparts. These exchange rates are, however, nicely correlated with the PAAP of the ligands as shown in Fig. 4. Moreover, as noted by Cavallo *et al.*,<sup>30</sup> there is an intriguing difference in  $\delta_{se}$  in the structurally similar unsaturated bis(aryl)NHCs (*e.g.* IMes **7** and IPr **9**) and we show here that this is reflected in the exchange rate of pyridine.

These examples demonstrate that the PAAP represents the best tool to analyse the electronic properties of NHC ligands and contributes in this case to a better understanding of the observed reactivity. It should be kept in mind, however, that this electronic effect is certainly not the only factor that influences the exchange rate of pyridine, and an exception to the general trend can be noted in Fig. 4. Ligand SiMnPr **3** has an exchange rate three times faster than its unsaturated counterpart ImNPr **4**, which is in line with the large difference in PAAP. The low absolute exchange rate of SiMnPr **3** can probably be attributed to the aliphatic nature of the R group and its relatively small buried volume. To illustrate the effect of buried volume further, IPr **9** was compared to the new IPent **10** catalyst. These imidazoliums with 2,6-substituted aryl groups exhibit similar  $\delta_{se}$  values (90 and 101 respectively), but IPent **10** has a significantly higher buried volume than IPr **9** (approx. 5% based on the Se crystal structure). Based on the general trend (exchange rate Py =  $0.12115(\delta_{se}) + 0.00246(\delta_{se})^2 + 4.28856$ ,  $R^2 = 0.99863$ ) an exchange rate of  $41.6 \text{ s}^{-1}$  is expected for IPent **10**, but in fact a much higher exchange rate, higher than that of any of the previously reported catalysts was observed, which must be explained by the much larger steric



bulk (see ESI† for details). These two examples illustrate that it is important to consider all properties of a ligand at all times.

## Conclusions

It is important to have a good understanding of the precise nature of the NHC-metal bond as control of the electronic and steric properties of NHC ligands can help in the design of significantly more active and selective catalyst systems. When the PAAP was introduced by Nolan, Cavallo and co-workers, it was predicted that this parameter would be suitable for more general use. Here we have shown that it indeed offers a tool to better understand the observed reactivity in a series of SABRE catalysts. The PAAP helps to explain, better than before, the observed difference in exchange rate of pyridine, which is crucial in the catalytic hyperpolarisation transfer process, between saturated and unsaturated NHC ligands. The parameter also gives insight in the remarkable difference in activity between the structurally similar ligands IMes **6** and IPr **9**. Although PAAP gives a more adequate description of electronic effects than TEP, it should be kept in mind that steric effects are also important as we have demonstrated in the case of 2,6-substituted aryl ligands. Ligands IPr **9** and IPent **10** have similar PAAP values, but steric properties control the observed reactivity. To conclude, the PAAP is a valuable new addition to the current set of parameters to characterise the electronic and steric properties of NHC ligands and offers more insight in the reactivity of NHC-metal catalysts in general.

## Acknowledgements

We thank the European Union (EFRD, European Fund for Regional Development) and the provinces of Gelderland and Overijssel for financially supporting the Ultrasense NMR project. The authors kindly thank Ad Swolfs and Ruud Aspers for their assistance with the <sup>77</sup>Se NMR experiments, and Paul Tinnemans for performing the X-ray crystallographic analysis.

## Notes and references

- R. W. Adams, J. A. Aguilar, K. D. Atkinson, M. J. Cowley, P. I. Elliott, S. B. Duckett, G. G. Green, I. G. Khazal, J. López-Serrano and D. C. Williamson, *Science*, 2009, **323**, 1708–1711.
- R. W. Adams, S. B. Duckett, R. A. Green, D. C. Williamson and G. G. R. Green, *J. Chem. Phys.*, 2009, **131**, 194505.
- S. Glöggl, R. Müller, J. Colell, M. Emondts, M. Dabrowski, B. Blümich and S. Appelt, *Phys. Chem. Chem. Phys.*, 2011, **13**, 13759.
- R. E. Mewis, R. A. Green, M. C. R. Cockett, M. J. Cowley, S. B. Duckett, G. G. R. Green, R. O. John, P. J. Rayner and D. C. Williamson, *J. Phys. Chem. B*, 2015, **119**, 1416–1424.
- E. B. Dücker, L. T. Kuhn, K. Münnemann and C. Griesinger, *J. Magn. Reson.*, 2012, **214**, 159–165.
- L. S. Lloyd, R. W. Adams, M. Bernstein, S. Coombes, S. B. Duckett, G. G. R. Green, R. J. Lewis, R. E. Mewis and C. J. Sleight, *J. Am. Chem. Soc.*, 2012, **134**, 12904.
- H. Zeng, J. Xu, J. Gillen, M. T. McMahon, D. Artemov, J.-M. Tyburn, J. A. B. Lohman, R. E. Mewis, K. D. Atkinson, G. G. R. Green, S. B. Duckett and P. C. M. van Zijl, *J. Magn. Reson.*, 2013, **237**, 73–78.
- S. Glöggl, M. Emondts, J. Colell, R. Müller, B. Blümich and S. Appelt, *Analyst*, 2011, **136**, 1566.
- N. Eshuis, N. Hermkens, B. J. A. van Weerdenburg, M. C. Feiters, F. P. J. T. Rutjes, S. S. Wijmenga and M. Tessari, *J. Am. Chem. Soc.*, 2014, **136**, 2695–2698.
- N. Eshuis, B. J. A. van Weerdenburg, M. C. Feiters, F. P. J. T. Rutjes, S. S. Wijmenga and M. Tessari, *Angew. Chem., Int. Ed.*, 2015, **54**, 1481–1484.
- J.-B. Hövener, N. Schwaderlapp, R. Borowiak, T. Lickert, S. B. Duckett, R. E. Mewis, R. W. Adams, M. J. Burns, L. A. R. Highton, G. G. R. Green, A. Olaru, J. Hennig and D. von Elverfeldt, *Anal. Chem.*, 2014, **86**, 1767–1774.
- A. N. Pravidtsev, A. V. Yurkovskaya, H.-M. Vieth and K. L. Ivanov, *Phys. Chem. Chem. Phys.*, 2014, **16**, 24672–24675.
- T. Theis, M. Truong, A. M. Coffey, E. Y. Chekmenev and W. S. Warren, *J. Magn. Reson.*, 2014, **248**, 23–26.
- D. A. Barskiy, K. V. Kovtunov, I. V. Koptuyug, P. He, K. A. Groome, Q. A. Best, F. Shi, B. M. Goodson, R. V. Shchepin, A. M. Coffey, K. W. Waddell and E. Y. Chekmenev, *J. Am. Chem. Soc.*, 2014, **136**, 3322–3325.
- M. Fekete, C. Gibard, G. J. Dear, G. G. R. Green, A. J. J. Hooper, A. D. Roberts, F. Cisnetti and S. B. Duckett, *Dalton Trans.*, 2015, **44**, 7870–7880.
- H. Zeng, J. Xu, M. T. McMahon, J. A. B. Lohman and P. C. M. van Zijl, *J. Magn. Reson.*, 2014, **246**, 119–121.
- M. L. Truong, F. Shi, P. He, B. Yuan, K. N. Plunkett, A. M. Coffey, R. V. Shchepin, D. A. Barskiy, K. V. Kovtunov, I. V. Koptuyug, K. W. Waddell, B. M. Goodson and E. Y. Chekmenev, *J. Phys. Chem. B*, 2014, **118**, 13882–13889.
- F. Shi, A. M. Coffey, K. W. Waddell, E. Y. Chekmenev and B. M. Goodson, *Angew. Chem., Int. Ed.*, 2014, **53**, 7495–7498.
- F. Shi, A. M. Coffey, K. W. Waddell, E. Y. Chekmenev and B. M. Goodson, *J. Phys. Chem. C*, 2015, **119**, 7525–7533.
- B. J. A. van Weerdenburg, S. Glöggl, N. Eshuis, A. H. J. Engwerda, J. M. M. Smits, R. de Gelder, S. Appelt, S. S. Wijmenga, M. Tessari, M. C. Feiters, B. Blümich and F. P. J. T. Rutjes, *Chem. Commun.*, 2013, **49**, 7388–7390.
- M. J. Cowley, R. W. Adams, K. D. Atkinson, M. C. R. Cockett, S. B. Duckett, G. G. R. Green, J. A. B. Lohman, R. Kerssebaum, D. Kilgour and R. E. Mewis, *J. Am. Chem. Soc.*, 2011, **133**, 6134–6137.
- M. Fekete, O. Bayfield, S. B. Duckett, S. Hart, R. E. Mewis, N. Pridmore, P. J. Rayner and A. Whitwood, *Inorg. Chem.*, 2013, **52**, 13453–13461.
- L. S. Lloyd, A. Asghar, M. J. Burns, A. Charlton, S. Coombes, M. J. Cowley, G. J. Dear, S. B. Duckett, G. R. Genov, G. G. R. Green, L. A. R. Highton,



- A. J. J. Hooper, M. Khan, I. G. Khazal, R. J. Lewis, R. E. Mewis, A. D. Roberts and A. J. Ruddlesden, *Catal. Sci. Technol.*, 2014, **4**, 3544–3554.
- 24 K. D. Atkinson, M. J. Cowley, P. I. P. Elliott, S. B. Duckett, G. G. R. Green, J. López-Serrano and A. C. Whitwood, *J. Am. Chem. Soc.*, 2009, **131**, 13362–13368.
- 25 A. J. Holmes, P. J. Rayner, M. J. Cowley, G. G. R. Green, A. C. Whitwood and S. B. Duckett, *Dalton Trans.*, 2015, **44**, 1077–1083.
- 26 H. Clavier and S. P. Nolan, *Chem. Commun.*, 2010, **46**, 841.
- 27 A. Poater, B. Cosenza, A. Correa, S. Giudice, F. Ragone, V. Scarano and L. Cavallo, *Eur. J. Inorg. Chem.*, 2009, **2009**, 1759.
- 28 R. A. Kelly III, H. Clavier, S. Giudice, N. M. Scott, E. D. Stevens, J. Bordner, I. Samardjiev, C. D. Hoff, L. Cavallo and S. P. Nolan, *Organometallics*, 2007, **27**, 202.
- 29 H. Jacobsen, A. Correa, A. Poater, C. Costabile and L. Cavallo, *Coord. Chem. Rev.*, 2009, **253**, 687–703.
- 30 S. V. C. Vummaleti, D. J. Nelson, A. Poater, A. Gomez-Suarez, D. B. Cordes, A. M. Z. Slawin, S. P. Nolan and L. Cavallo, *Chem. Sci.*, 2015, **6**, 1895–1904.

